Mettl3-mediated m[6]A modification plays a role in lipid metabolism disorders and progressive liver damage in mice by regulating lipid metabolism-related gene expression

Guanqi Dai[1,6,*], Shihao Huang[1,*], Yonglong Li[1,2,*], Xueyi Tu[1,*], Jiawei Xia[3,*], Zhihao Zhou[1], Wanyi Chen[1], Ao Zhang[1], Jintao Lin[1], Yingchun Li[1], Danhua He[1], Taoyan Lin[4], Jinge Cong[1,2], Ye Lei[1,2], Liuxin Han[3], Zhenxia Yao[1], Weiwei Liu[1], Ying Zhou[1], Qiwen Li[1], Jing Li[5], Yuqin Zhang[6], Aibing Wu[7], Dong Xiao[1,2], Wanshan Wang[2], Wentao Zhao[1,8], Junshuang Jia[1], Xiaolin Lin[9]

[1]Cancer Research Institute, Experimental Education/Administration Center, School of Basic Medical Sciences, Southern Medical University, Guangzhou 510515, China
[2]Laboratory Animal Management Center, Southern Medical University, Guangzhou 510515, China
[3]The Third People's Hospital of Kunming (The Sixth Affiliated Hospital of Dali University), Kunming 650041, China
[4]Department of Pharmacy, Nanfang Hospital, Southern Medical University, Guangzhou 510515, China
[5]Radiotherapy Center, The First People's Hospital of Chenzhou, Xiangnan University, Chenzhou 423000, China
[6]Department of Radiation Oncology, Nanfang Hospital, Southern Medical University, Guangzhou 510515, China
[7]Department of Oncology, The Central People's Hospital of Zhanjiang, Zhanjiang 524000, China
[8]Department of Gastrointestinal Oncology, The Third Affiliated Hospital of Kunming Medical University (Yunnan Cancer Hospital, Yunnan Cancer Center), Kunming 650118, China
[9]Cancer Center, Integrated Hospital of Traditional Chinese Medicine, Southern Medical University, Guangzhou 510315, China
*Equal contribution

Correspondence to: Dong Xiao, Xiaolin Lin, Junshuang Jia, Wentao Zhao, Wanshan Wang; email: xiaodong@smu.edu.cn, lxl0644@smu.edu.cn, jiajsh4@smu.edu.cn, zhaowentao@kmmu.edu.cn, wws@smu.edu.cn

ABSTRACT

Aims: N6-methyladenosine (m[6]A), the most abundant and conserved epigenetic modification of mRNA, participates in various physiological and pathological processes. However, the roles of m[6]A modification in liver lipid metabolism have yet to be understood entirely. We aimed to investigate the roles of the m[6]A "writer" protein methyltransferase-like 3 (Mettl3) in liver lipid metabolism and the underlying mechanisms.

Main Methods: We assessed the expression of Mettl3 in liver tissues of diabetes (db/db) mice, obese (ob/ob) mice, high saturated fat-, cholesterol-, and fructose-induced non-alcoholic fatty liver disease (NAFLD) mice, and alcohol abuse and alcoholism (NIAAA) mice by quantitative reverse-transcriptase PCR (qRT-PCR). Hepatocyte-specific Mettl3 knockout mice were used to evaluate the effects of Mettl3 deficiency in mouse liver. The molecular mechanisms underlying the roles of Mettl3 deletion in liver lipid metabolism were explored by multi-omics joint analysis of public data from the Gene Expression Omnibus database and further validated by qRT-PCR and Western blot.

Key Findings: Significantly decreased Mettl3 expression was associated with NAFLD progression. Hepatocyte-specific knockout of Mettl3 resulted in significant lipid accumulation in the liver, increased serum total cholesterol levels, and progressive liver damage in mice. Mechanistically, loss of Mettl3 significantly downregulated the expression levels of multiple m⁶A-modified mRNAs related to lipid metabolism, including Adh7, Cpt1a, and Cyp7a1, further promoting lipid metabolism disorders and liver injury in mice.

Significance: In summary, our findings demonstrate that the expression alteration of genes related to lipid metabolism by Mettl3-mediated m⁶A modification contributes to the development of NAFLD.

INTRODUCTION

The liver is an essential organ with complex functions, including metabolism, drug detoxification, and hormone secretion [1]. It plays a central role in lipid homeostasis, including the synthesis of new fatty acids, uptake of circulating fatty acids, biosynthesis of triglycerides, and fatty acid oxidation [2], and disruption of one or more of these pathways may cause lipid metabolism disorder, which is a major contributing factor to cardiovascular diseases and nonalcoholic fatty liver disease (NAFLD) [3]. Recently, increasing evidence has shown that hepatic cholesterol accumulation, characterized by elevated cholesterol synthesis, uptake from circulating lipoproteins, and reduced cholesterol excretion, contributes to the pathogenesis of NAFLD [4–6]. Thus, identifying the key regulators of lipid metabolism may provide effective treatment measures for NAFLD.

The critical role of epigenetic modifications in metabolic diseases has been widely reported [7, 8]. Among these medications, the N6-methyladenosine (m⁶A) modification is the most prevalent internal modification of mRNAs. It is catalyzed by a series of m⁶A "writers," such as methyltransferase-like 3 (Mettl3) [9], Mettl14 [10], Mettl16 [11], and Wilms tumor 1-associated protein (WTAP) [12]. It can be removed by RNA demethylases, including fat mass and obesity-associated protein (FTO) [13] and alkylation repair homolog protein 5 (ALKBH5) [14]. This modification can be recognized by a set of YHT family domain-containing "reader" proteins (Ythdf1/2/3) [15, 16] or insulin-like growth factor-2 mRNA-binding proteins (Igfbp1/2/3) [17] and regulates gene expression by affecting multiple aspects of mRNA metabolism, such as RNA splicing, RNA stability, and mRNA translation efficiency [18]. Mettl3-mediated m⁶A modification plays a role in multiple biological events and complex diseases, such as spermatogenesis [19], stem cell pluripotency [20], postnatal liver development [21], and tumorigenesis [22]. Moreover, Mettl3 regulates lipid metabolism in the liver and participates in NAFLD progression [23–25]. However, the molecular mechanisms underlying Mettl3-mediated regulation of liver lipid metabolism and NAFLD progression have not been fully elucidated.

The present study aimed to investigate the roles of Mettl3 in liver lipid metabolism using Mettl3 hepatocyte-specific knockout (HKO) mice and multi-omics joint analysis of public data from the Gene Expression Omnibus (GEO) database. Our study revealed that Mettl3 deficiency in hepatocytes mediated m⁶A modification regulated lipid metabolism and non-alcoholic fatty liver disease (NAFLD) progression by significantly downregulating genes related to lipid metabolism. The newly identified lipid metabolism-related genes modified by Mettl3-mediated m⁶A modification may serve as potential targets for the treatment of NAFLD in the future.

RESULTS

Mettl3 expression is downregulated in liver tissues of patients and mice with obesity

To determine the expression of Mettl3 in fatty liver, we first used a public gene expression dataset from the GEO database. We found that the mRNA expression of Mettl3 was significantly decreased in the liver of patients with obesity compared to that in lean individuals (Figure 1A). To further uncover the expression of Mettl3 with the progression of NAFLD, we analyzed the expression correlation of Mettl3 with Cd36 and Dgat1. As previously reported, the expression of Cd36 in the liver positively correlates with the progression of morbidly obese patients [26]. Dgat1 is a critical enzyme in triglyceride synthesis and NAFLD development [27–29]. Pearson's correlation analysis revealed that the expression of Mettl3 in the liver was significantly negatively correlated with Cd36 and Dgat1 (Figure 1B and Supplementary Figure 1). Moreover, quantitative reverse transcriptase PCR (qRT-PCR) analysis revealed that the mRNA level of Cd36 was significantly upregulated in the liver of four different kinds of fatty liver disease mouse models (Figure 1C–1F). However, Mettl3 expression was significantly down-regulated in the liver of diabetes (db/db) mice and obese (ob/ob) mice (Figure 1C, 1D) but not in the liver of alcohol abuse and alcoholism (NIAAA) mice and high saturated fat, cholesterol, and fructose (FFC) diets induced mice (Figure 1E, 1F) compared to the control. These results indicate that the downregulation of Mettl3 expression in the livers may be associated with specific fatty liver disease pathogenesis.

Mettl3 HKO induces lipid accumulation in mouse hepatocytes

To further determine the exact roles of Mettl3 in the progression of fatty liver disease, we crossed Mettl3^flox/flox mice with heterozygous Alb-Cre mice to obtain Mettl3^flox/wt; Alb-Cre mice (Figure 2A).

We further intercrossed Mettl3^flox/wt; Alb-Cre mice with Mettl3^flox/flox mice to obtain Mettl3^flox/flox; Alb-Cre mice (Figure 2B). The mice eventually used in the experiments were obtained by intercrossing Mettl3^flox/flox; Alb-Cre with Mettl3^flox/flox mice (Figure 2C). The hepatocyte-specific knockout of Mettl3 was validated by agarose gel electrophoresis using
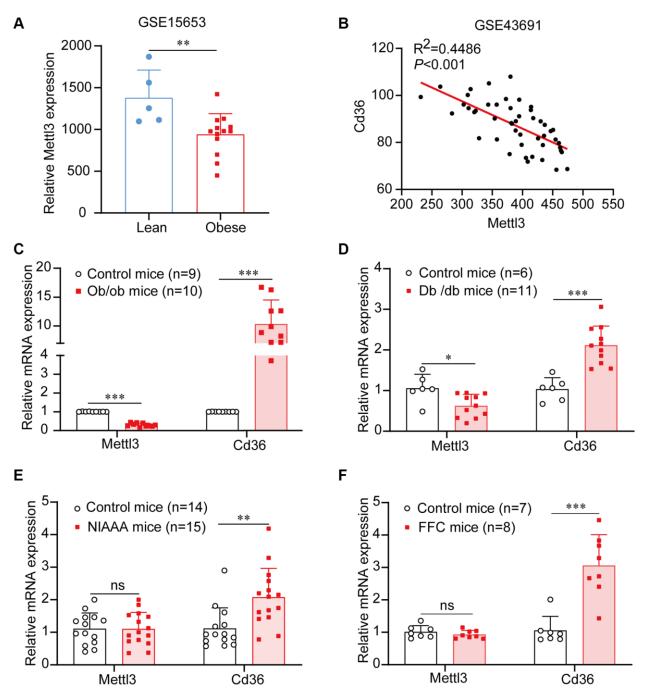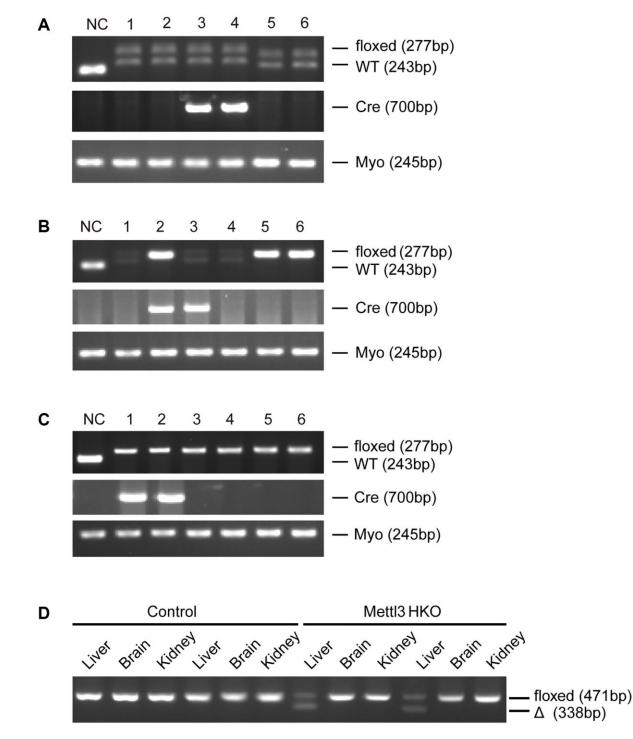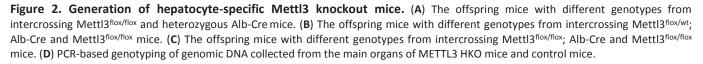
Figure 1. Mettl3 expression is downregulated in liver tissues of patients and mice with obesity. (**A**) Mettl3 expression is downregulated in the liver of patients with obesity (with or without type 2 diabetes) compared to that in lean individuals from the GEO dataset (GSE15653). (**B**) The expression of Mettl3 is significantly negatively correlated with Cd36 in liver of obese hyperphagic mice fed with the high-fat diet and control mice from the GEO dataset (GSE43691). (**C–F**) Relative expression of Mettl3 in the livers of ob/ob (**C**), db/db (**D**), NIAAA (**E**), and FFC (**F**) mice was detected by qRT-PCR. Data are presented as the mean ± SD. Abbreviation: ns: not significant; $^*P < 0.05$; $^{**}P < 0.01$; $^{***}P < 0.001$.

liver, brain, and kidney tissues (Figure 2D). Moreover, qRT-PCR and Western blotting confirmed that the expression of Mettl3 was dramatically reduced in the liver of Mettl3 HKO mice (Figure 3A, 3B). To determine the function of Mettl3 in the liver, we dissected the livers of Mettl3 HKO and control mice at 4 and 12 weeks. The body weight (Figure 3C), liver weight (Figure 3D), and liver-to-body weight ratio (Figure 3E) were comparable between Mettl3 HKO and control mice at both 4 and 12 weeks. However, the mouse liver in the Mettl3 HKO group showed a more yellowish appearance than in the control group at

Figure 2. Generation of hepatocyte-specific Mettl3 knockout mice. (**A**) The offspring mice with different genotypes from intercrossing Mettl3$^{flox/flox}$ and heterozygous Alb-Cre mice. (**B**) The offspring mice with different genotypes from intercrossing Mettl3$^{flox/wt}$; Alb-Cre and Mettl3$^{flox/flox}$ mice. (**C**) The offspring mice with different genotypes from intercrossing Mettl3$^{flox/flox}$; Alb-Cre and Mettl3$^{flox/flox}$ mice. (**D**) PCR-based genotyping of genomic DNA collected from the main organs of METTL3 HKO mice and control mice.

4 weeks. This difference became more pronounced at 12 weeks (Figure 3F). Consistent with this, H&E staining of mouse liver tissues at 12 weeks showed diffuse microsteatosis of hepatocytes (Figure 3F). Furthermore, Oil Red O staining indicated that large red lipid droplets were deposited in hepatocytes at both
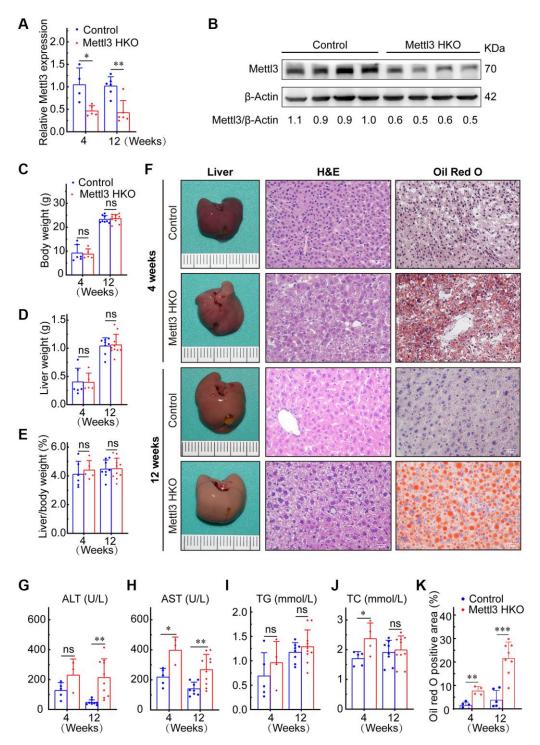

Figure 3. Hepatocyte-specific deletion of Mettl3 induces lipid accumulation in mouse liver cells. (**A**) qRT-PCR assay of the relative Mettl3 expression in control and METTL3 HKO mouse livers at 4 and 12 weeks. (**B**) Representative Western blot analysis and quantitative results in control and METTL3 HKO mouse livers. (**C–F**) Body weight (**C**), liver weight (**D**), and liver-to-body weight ratio (**E**) of METTL3 HKO and control mice at 4 and 12 weeks. (**F**) Representative images of the livers of METTL3 HKO (n = 5 for 4 weeks; n = 10 for 12 weeks) and control mice (n = 6 for 4 weeks; n = 8 for 12 weeks) stained with hematoxylin and eosin and Oil red O. Scale bars, 25 μm. (**G–K**) Serum levels of ALT (**G**), AST (**H**), TG (**I**), TC (**J**), and Oil red O positive area (**K**). Data are presented as mean ± SD. Abbreviations: TG: triglyceride; TC: total cholesterol; ns: not significant; *$P < 0.05$; **$P < 0.01$; ***$P < 0.001$.

timepoints (Figure 3F, 3K). In conclusion, these results suggested lipid accumulation in the hepatocytes of METTL3 HKO mice.

Mettl3 HKO induces lipid metabolism disorder and liver injury

Mettl3 HKO mice also showed higher serum alanine aminotransferase (ALT) activities at 4 and 12 weeks (Figure 3G). Serum aspartate transaminase (AST) activity was also significantly increased in Mettl3 HKO mice at both time points compared to that in control mice, and the difference was more pronounced at 12 weeks (Figure 3H). These results indicate that the hepatocyte deletion of Mettl3 results in progressive liver injury. We also observed a significant increase in serum total cholesterol (TC) levels in the METTL3 HKO group at 4 weeks (Figure 3J). Although the triglyceride (TG) level was slightly elevated in the METTL3 HKO group, it did not reach statistical significance at either time points (Figure 3I). Collectively, these results indicate that knockout of Mettl3 induced lipid dysmetabolism and caused liver injury in mice.

Mettl3 HKO results in the downregulation of lipid metabolism-related gene expression

To reveal the molecular events underlying the effect of Mettl3 knockout on lipid metabolism, we analyzed a publicly available gene expression dataset of METTL3 HKO liver from the GEO database (GSE176113). PCA plot showed good reproducibility among the replicates of each group and apparent differences between the two groups (Figure 4A). Moreover, 826 protein-coding genes were upregulated, and 528 protein-coding genes down-regulated significantly upon METTL3 HKO in this dataset (adjust-$P < 0.05$, fold change >1.5; Figure 4B). Gene set enrichment analysis (GSEA) using the curated gene set compilation M5 (MSigDb M5) demonstrated that several lipid metabolism and transport related-gene sets, including cellular lipid catabolic process, fatty acid beta-oxidation, cholesterol biosynthetic process, and cholesterol efflux, were significantly suppressed under the METTL3 HKO condition (|normalized enrichment score|>2.0; Figure 4C–4F), which may attribute to the phenotype of increased liver lipid accumulation and elevated serum cholesterol level in the METTL3 HKO mice. Moreover, several apoptosis and cell cycle-related gene sets were significantly positively enriched under the METTL3 HKO condition (|normalized enrichment score |>1.5; Figure 4G, 4H). These results indicate that METTL3 HKO caused lipid accumulation and subsequent apoptosis of hepatocytes, further leading to the compensatory proliferation of hepatocytes.

Multiple omics analyses identify the specific targets of lipid disorder caused by Mettl3-mediated m⁶A modification

To gain deeper insights into the molecular mechanism underlying the effects of Mettl3 HKO on liver lipid metabolism, we overlapped significantly demethylated genes (GSE142835) (|fold change|>2) with significantly downregulated genes under the Mettl3 HKO condition (GSE176113) (|fold change|>1.5) as well as genes related to lipid metabolism and transport. A total of 12 genes were identified (Figure 5A). The four-quadrant diagram showed that these genes were dramatically hypomethylated and downregulated (Figure 5B). The hypomethylation levels of these genes under the Mettl3 HKO condition were further validated by the GSE179680 dataset (data not shown). Cholesterol 7α-hydroxylase (Cyp7a1), which is involved in the catalysis of cholesterol synthesis of bile acids, and ATP-binding cassette subfamily G member 8 (Abcg8), which mediates hepatic cholesterol efflux, were dramatically hypomethylated in the Mettl3 HKO group (Figure 5C, 5D). In addition, most of these genes, including Cyp7a1 and Abcg8, had classical m⁶A "DRACH" motifs in the 3′UTR or near the stop codon (Figure 5E, 5F). Meanwhile, Ahd7 and Cpt1a, key enzymes in fatty acid oxidation [30, 31], were significantly demethylated in the liver of Mettl3 HKO mice (Figure 6A, 6B). Structurally, both Adh7 and Cpt1a have the classic "DRACH" sequence on the last exon (Figure 6C, 6D). These results indicate that Mettl3 may regulate lipid metabolism in hepatocytes by downregulating the expression of these lipid metabolism genes via m⁶A modification.

Genes related to lipid metabolism are significantly downregulated in the liver of METTL3 HKO mice

We performed qRT-PCR to validate our hypothesis that Mettl3 regulates the expression of lipid metabolism-related genes via m⁶A modification. As expected, most of the genes related to fatty acid oxidation (Figure 7A), cholesterol efflux (Figure 7B), lipid metabolic process (Figure 7C), lipid transport (Figure 7D), and lipid biosynthetic process (Figure 7E) were significantly decreased in the livers of Mettl3 HKO mice. Moreover, we found an expression correlation of the potential target genes with Mettl3 (Supplementary Figure 2) using the GEO database. Furthermore, the protein expression of Adh7, Cpt1a, and Cyp7a1 was significantly downregulated in the liver of METTL3 HKO mice. While the expression of Abcg8 and Hmgcr remains unchanged between the two groups (Figure 7F, 7G). The significant downregulation of Adh7 and Cpt1a could further lead to decreased hepatocyte fatty acid oxidation, while the apparent downregulation of Cyp7a1 could decrease the conversion and transport of cholesterol in the liver. In conclusion, these results

suggested that hepatocyte-specific Mettl3 deficiency-mediated significant downregulation of Adh7, Cpt1a, and Cyp7a1 may account for lipid accumulation and elevated serum cholesterol amounts in mice (Figure 8).

DISCUSSION

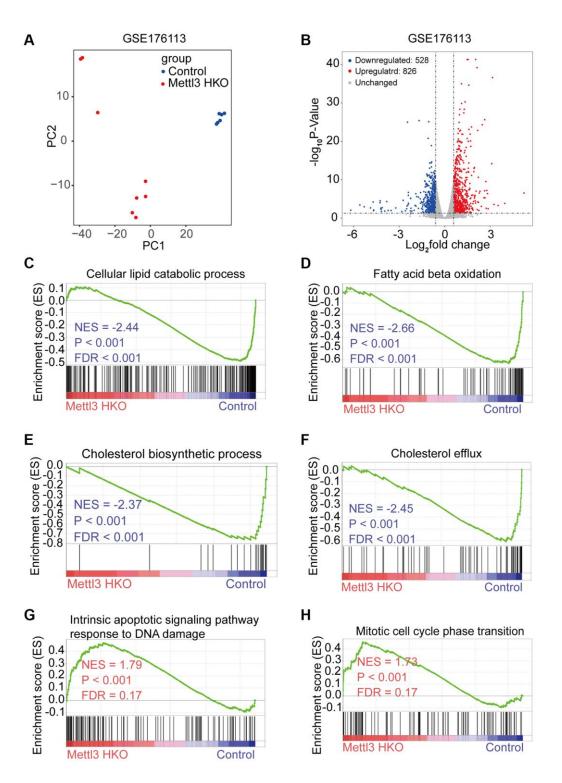Currently, NAFLD is a significant global health problem with no approved treatments. Dysfunction of

Figure 4. Specific knockout of Mettl3 in hepatocytes results in downregulating lipid metabolism-related genes. (**A**) Principal component analysis (PCA) plot showing reproducibility among the replicates of each group. (**B**) Volcano plot showing the differential expression of protein-coding genes in the GSE176113 dataset. (**C–H**) Gene set enrichment analysis (GSEA) plot of enrichment of indicated signatures in Mettl3 HKO livers using the C5 MSigDB database.

liver lipid metabolism plays a vital role in the progression of NAFLD. However, the molecular mechanisms of liver lipid metabolism mediated by epigenetics have yet to be entirely understood. The present study found that decreased Mettl3 expression in NAFLD mouse models was associated with liver metabolic disorders. Using Mettl3 HKO mice, we observed significant lipid accumulation in the
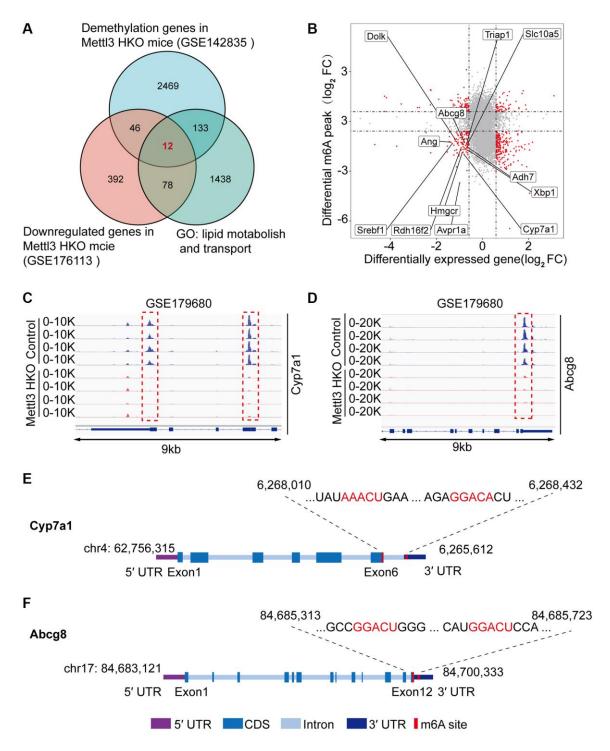

Figure 5. Multiple omics analyses identify the specific targets of lipid disorder caused by Mettl3-mediated m⁶A modification. (**A**) Venn diagram showing the number of overlapping Hypo-m6A-methylated mRNAs and downregulated genes in the liver of METTL3 HKO mice. Then the resultant 58 genes were annotated to GO term lipid metabolism and transport and obtained 12 genes. (**B**) Four-quadrant diagram showing the differentially methylated genes and differentially expressed genes in GSE142835 and GSE176113. (**C**, **D**) Peak distribution normalized to input in the genomic regions of Cyp7a1 (**C**) and Abcg8 (**D**) in control and METTL3 HKO mice in the GSE179680 dataset is shown. (**E**, **F**) Schematic representation of predicted positions of m6A motifs within Cyp7a1 (**E**) and Abcg8 (**F**) mRNA.

hepatocytes at 4 and 12 weeks. Moreover, increased serum levels of TC and progressive liver damage were observed in Mettl3 HKO mice compared to those in normal control mice at 4 and 12 weeks. Using public data from GEO for a multi-omics joint analysis and further molecular biology experiments, we identified potential targets modified by Mettl3-mediated m6A modification, such as Adh7, Cpt1a, and Cyp7a1, which regulate liver lipid metabolism. These results offer new insights into the molecular mechanism of m6A modifications in liver metabolism and may serve as a potential therapeutic target.

Previous studies have shown that the loss of Mettl3 in hepatocytes promotes lipid accumulation in the liver and contributes to the progression of NAFLD [21, 23, 24]. However, the exact molecular mechanism is not fully understood. The nuclear protein level of Mettl3 is significantly decreased in the liver of methionine-

choline-deficient diet-induced nonalcoholic steato-hepatitis (NASH) mice and patients with NASH but significantly increased in the liver of high-fat diet-induced NASH mice [23]. In our study, Mettl3 mRNA expression was significantly downregulated in the livers of db/db and ob/ob mice but kept unchanged in the livers of NIAAA and FFC mice. These results were seemingly contradictory. However, owing to the different etiology of fatty liver disease caused by different molecular mechanisms, Mettl3 may participate in the pathogenesis of fatty liver disease related to glucose metabolism disorders.

The present study found that hepatocyte Mettl3 knockout resulted in lipid accumulation in the liver, elevated serum TC levels, and progressive liver injury, consistent with a previous report [21]. The high amount of TG accumulation in the liver may be caused by the significant downregulation of genes involved in
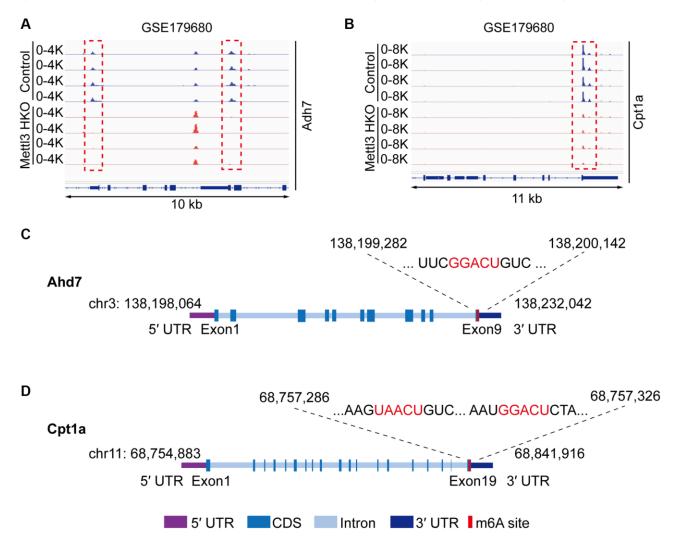

Figure 6. Adh7 and Cpt1a are the potential targets modified by Mettl3-mediated m6A modification in regulating liver lipid metabolism. (**A**, **B**) Peak distribution normalized to input in the genomic regions of Adh7 (**A**) and Cpt1a (**B**) in control and METTL3 HKO mice in the GSE179680 dataset. (**C**, **D**) Schematic representation of predicted positions of m6A motifs within Adh7 (**C**) and Cpt1a (**D**) mRNA.

lipid catabolic processes and fatty acid oxidation, such as Adh7 and Cpt1a. As a critical ethanol-metabolizing enzyme, Adh7 participates in fatty acid omega-oxidation [31]. However, the roles of Adh7 in NAFLD and its epigenetic regulation by m6A modification have yet to be reported. Our study suggested that significant downregulation of Adh7 expression, regulated by Mettl3-mediated m6A modification, may contribute to
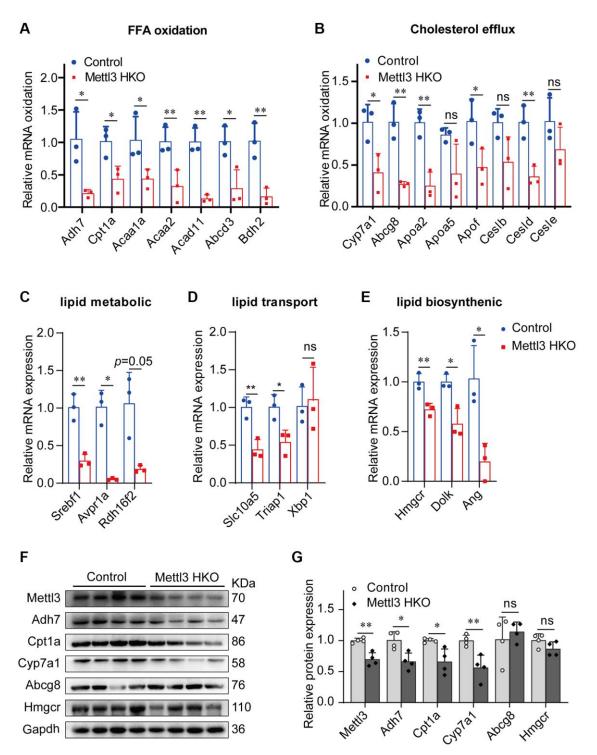

Figure 7. Genes related to lipid metabolism are significantly downregulated in the liver of METTL3 HKO mice. (**A–E**) qRT-PCR analysis of the mRNA expression of genes related to fatty acid oxidation (**A**), cholesterol efflux (**B**), lipid metabolic process (**C**), lipid transport (**D**), and lipid biosynthetic process (**E**) in the liver of METTL3 HKO mice and control mice. (**F–G**) Representative immunoblotting images (**F**) and quantitative results (**G**) for the potential target gene in the liver of METTL3 HKO mice and control mice. Data are presented as the mean ± SD. Abbreviations: FFA: free fatty acid; ns: not significant; $^*P < 0.05$; $^{**}P < 0.01$.

NAFLD progression. Meanwhile, Cpt1a is a critical enzyme in fatty acid beta-oxidation, whose mRNA was also significantly demethylated around the stop codon in the liver of Mettl3 HKO mice. Moreover, the mRNA and protein expression of Cpt1a was also dramatically downregulated under the Mettl3 HKO condition. Therefore, this gene is likely to be regulated by Mettl3-mediated m^{6}A modification and thus participate in forming the fatty liver caused by Mettl3 knockout. In addition, the significant increase in serum TC in our study may be caused by the combined effect of multiple genes related to cholesterol metabolism, including Cyp7a1, which plays a fundamental role in the regulation of hepatic cholesterol homeostasis by converting excess cholesterol to bile acids [32] and mediating cholesterol excretion via bile [33, 34]. In the present study, Cyp7a1 was significantly hypo-methylated and downregulated, leading to decreased conversion and cholesterol transport into bile. These multiple effects eventually lead to a significant increase in serum cholesterol levels in Mettl3 HKO mice. Although a previous study has demonstrated the importance of cholesterol metabolism in NAFLD progression, few studies have reported the regulatory mechanism of cholesterol metabolism by m^{6}A modification. Our study demonstrated, for the first time, that genes related to cholesterol metabolism, including Cyp7a1, may participate in NAFLD progression through Mettl3-mediated m^{6}A modification.

In addition, there were nine other lipid metabolism-related genes, including Abcg8, Hmgcr, Srebf1, Triap1, Avpr1a, Dolk, Rdh16f2, Slc10a5, and Ang, which significantly lost their m^{6}A modification and were downregulated in Mettl3 HKO mice. In these genes, Abcg8 worked as an essential enzyme mediating cholesterol excretion via bile [35]. Hmgcr is the enzyme catalyzing the rate-limiting step of cholesterol biosynthesis [36]. These genes were significantly downregulated at the mRNA level but kept unchanged at the protein level in METTL3 HKO mouse livers. Thus, their effect on NAFLD formation needs further study to illustrate. Srebf1 is a membrane-bound transcription factor that affects multiple biological processes of lipid homeostasis, including the synthesis of fatty acids, triglycerides, and cholesterol. Although the decreased expression of Srebf1 does not match the phenotype of hepatic lipid accumulation under the Mettl3 HKO condition, it may participate in hepatic lipid accumulation induced by Mettl3 loss, while its roles have been overshadowed by other genes. Except for Abcg8, Hmgcr, and Srebf1, the other genes' roles in NAFLD need to be clarified. Thus, more profound studies are needed to clarify whether these genes contribute to the progression of NAFLD.

Our study has limitations. We did not validate Mettl3 protein expression in the liver of NAFLD mouse models and human NAFLD subjects. Moreover, the regulatory effect of m^{6}A modification on mRNA fate is determined
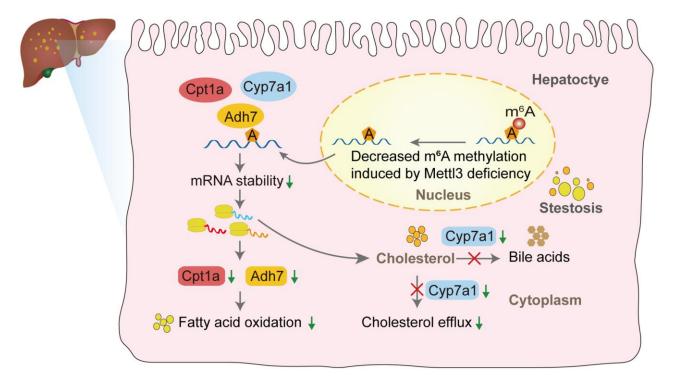

Figure 8. The proposed model of liver lipid accumulation through decreased m^{6}A modification of the lipid metabolism genes mediated by Mettl3 deficiency.

by a set of "reader" proteins after recognizing of m6A-modified transcripts, in which IGF2BP family proteins work to promote the stability of target mRNA [18]. Thus, we focused on genes significantly downregulated by Mettl3 HKO. However, if m6A modification is recognized by the "reader" protein YTHDF2 under Mettl3 HKO conditions, the expression of target genes is likely to be upregulated due to reduced degradation [37]. We also haven't identified the "reader" protein under the Mettl3 HKO condition. Hence, future studies should address these issues.

CONCLUSION

In summary, our study suggested the regulatory function of Mettl3-mediated epigenetic modification in mouse liver lipid metabolism, expanding our under-standing of the regulatory network outside of transcriptomics in mammalian liver lipid metabolism and NAFLD pathogenesis. The newly identified lipid metabolism-related target genes may be potential targets for the treatment of NAFLD in the future.

MATERIALS AND METHODS

Animal experiments

All mice used in this study were raised in a specific pathogen-free-grade facility under a 12-h light/12-h dark cycle at $24 \pm 2°C$ and humidity of $50\% \pm 10\%$. Mice were fed a standard chow diet with free access to water. All animal experiments were conducted in accordance with the National Institutes of Health Guide for the Care and Use of Laboratory Animals and were approved by the Animal Care and Use Committee of Southern Medical University.

Generation of Mettl3^{flox/flox}; Alb-Cre mice

Mettl3$^{flox/wt}$ mice were generated using CRISPR-Cas9 system-assisted homologous recombination. Mettl3$^{flox/flox}$ mice, in which exon 4 of Mettl3 was flanked by two loxp sites, were generated by mating Mettl3$^{flox/wt}$ and Mettl3$^{flox/wt}$ mice. The oligonucleotide sequences of the two sgRNAs were as follows: sgRNA1, GAAGTTACA CTCTTTTAGGGAGG; sgRNA2, TAAACACCGGCCC TACGCCCAGG. Alb-Cre mice were purchased from Cyagen Biosciences (Suzhou, China). Mettl3$^{flox/flox}$; Alb-Cre (Mettl3 HKO) mice were generated by crossing Mettl3$^{flox/flox}$ mice with Alb-Cre mice. Both male and female mice were used for further experiments.

Genotype analysis using PCR

Genomic DNA was prepared from mouse ear tissue using the TIANamp Genomic DNA Kit (Tiangen, Beijing, China), according to our previous publication [38]. Genotypes were determined by PCR using primers specific for Cre: 5′-ATCCGAAAAGAAAAC GTTGA-3′ (forward), 5′-ATCCAGGTTA CGGATATAGT-3′ (reverse); and specific for Mettl3: 5′-TAGTGCTGTGCCTTTCTTAG-3′ (Mettl3-L-LOXP-F), 5′-TTAAACTGACTGCCTCCATA-3′ (Mettl3-L-LOXP-R). The genomic DNA from a wild-type (WT) mice was used as a template. Moreover, to assess the knockout efficiency of Mettl3 in adult liver, the main organs and tissues DNA, including the liver was subjected to PCR using the following primer pair to amplify 338bp Mettl3 mutant fragment, F1: GTGCTGTGCCTTTCTTAG, R1: AGCGTCACTGG CTTTCAT, and R2: TTCTTGTTCTCCCCCAAT. Primer pairs for Myo were used as a negative control (forward primer: TTACGTCCATCGTGGACAGC, reverse primer: TGGGCTGGGTGTTAGCCTTA).

Mouse models of fatty liver disease

All mouse models of fatty liver disease were generated using age-appropriate male mice with a C57BL/6 genetic background. Diabetes (db/db) mice and obese (ob/ob) mice were purchased from GemPharmatech Co., Ltd. (Jiangsu, China) ($n = 11$ for db/db mice, $n = 10$ for ob/ob mice). The National Institute on Alcohol Abuse and Alcoholism (NIAAA) model ($n = 15$) was induced by chronic and binge ethanol feeding as previously described [39]. The high saturated fat, cholesterol, and fructose (FFC) mouse model ($n = 8$) were induced by feeding with high fructose, high-fat, and high-cholesterol diet (research Dies: D09100310) for 24 weeks as previously reported [40].

Histological analysis

Formalin-fixed, paraffin-embedded liver tissue samples were cut into 4 µm-thick sections and stained with hematoxylin and eosin (H&E) according to standard procedures. According to the manufacturer's instructions, liver lipid accumulation was confirmed using a Modified Oil Red O stain kit (Catalog No. C0158S; Beyotime, Beijing, China). Briefly, frozen liver slices (8 µm) were fixed in 10% formaldehyde for 10 min and then washed with 60% isopropanol for 20–30 s. Liver tissue was stained in Modified Oil Red O solution for 20 min. After staining, the slices were washed with 60% isopropanol and H_2O.

Serological test

The supernatant was obtained by centrifugation at 800 g for 10 min. The mouse serum levels of liver damage indices, blood lipids, and blood sugar were detected

using the Beckman automatic biochemical analyzer AU680 (Beckman Coulter, Brea, CA, USA).

RNA extraction and quantitative reverse transcriptase PCR

Total RNA was extracted from the mouse liver at the same anatomical position using TRIzol Reagent (TaKaRa) and reverse-transcribed into cDNA using the Reverse Transcription System (TaKaRa). qRT-PCR was performed using the SYBR Green qPCR Master Mix (TaKaRa) and a LightCycler 96 system (Roche). Relative gene expression was analyzed using the $2^{-\Delta\Delta Ct}$ method with Gapdh as the internal control. All primers used in this study are listed in Supplementary Table 1.

Western blotting

Total proteins from mouse liver tissues were extracted by Total Protein Extraction Kit (Keygen) and further quantified by BCA Protein Quantitation Kit (Keygen) according to the manufacturer's instructions. Western blotting was performed as previously described with the following primary antibodies: anti-Mettl3 (1:1000; ab195352; Abcam), anti-β-actin (1:2000, 20536-1-AP; Proteintech Group), anti-Gapdh (1:5000, 10494-1-AP; Proteintech Group), anti-Adh7 (1:1000; 23425-1-AP; Proteintech Group), anti-Cpt1a (1:1000; 15184-1-AP; Proteintech Group), anti-Cyp7a1 (1:500; sc-293193; Santa Cruz), anti-Hmgcr (1:500; sc-271595; Santa Cruz), and anti-Abcg8 (1:1000; A01482-1; Boster).

Public dataset

All the public datasets used in this study were obtained from the National Cancer for Biotechnology Information GEO. RNA transcriptome sequencing data were from patients with obesity (GSE15653) and Mettl3 HKO mice (GSE176113). The MeRIP-seq datasets GSE179680 and GSE142835 were from Mettl3-knockout livers. The results of principal component analysis (PCA), volcano map, four-quadrant diagram, and Venn diagram were visualized using the ggplot2 package [3.3.6]. GSEA was performed using GSEA software (version 4.3.2) downloaded from https://www.gsea-msigdb.org/gsea/index.jsp [41], using the curated gene set compilation M5 (MSigDb M5). The m6A modification peaks of target genes were visualized by Integrative Genomics Viewer (IGV) software (version 2.16.0) downloaded from https://igv.org/ [42]. The potential m6A sites ("DRACH," where D = A, G or U; R = A or G; H = A, C or U) of the target genes were predicted using an online tool, SRAMP (http://www.cuilab.cn/sramp/) [43].

Statistical analysis

Student's *t*-test was used to compare two groups if the data met the normal distribution; otherwise, the Mann-Whitney *U* test was used. GraphPad Prism software (version 8.0) was used to analyze all data. Statistical significance was set at $P < 0.05$. Data are expressed as mean ± SD.

Data availability

The data supporting this study's findings are available from the corresponding author upon reasonable request.

AUTHOR CONTRIBUTIONS

X. L. Lin, W.T. Zhao, J.S. Jia, W.S. Wang, and D. Xiao: Conceived and designed the experiments. Y.L. Li, S.H Huang, G.Q. Dai, X.Y. Tu, W.Y. Chen, J.T. Lin, Y.C. Li, J.G. Cong, Z.X. Yao, W.W. Liu, A. Zhang, and Y.Q. Zhang: Performed the experiments. G.Q. Dai and Z.H. Zhou: Performed the bioinformatics analyses. G.Q. Dai: Analyzed the data. D.H. He, T.Y. Lin, Y. Lei, Y. Zhou, Q.W. Li, J. Li, J.W. Xia, L.X. Han, A.B. Wu, Y.Q. Zhang, and W.S. Wang: Contributed reagents/materials/analysis tools. G.Q. Dai and D. Xiao: Wrote the manuscripts. D. Xiao and X. L. Lin：Advice and comments, general and administrative support. All the authors read and approved this paper.

CONFLICTS OF INTEREST

The authors declare no conflicts of interest related to this study.

ETHICAL STATEMENT

All animal experiments were conducted in accordance with the National Institutes of Health Guide for the Care and Use of Laboratory Animals and were approved by the Animal Care and Use Committee of Southern Medical University.

REFERENCES

1. Ober EA, Lemaigre FP. Development of the liver: Insights into organ and tissue morphogenesis. J Hepatol. 2018; 68:1049–62.
https://doi.org/10.1016/j.jhep.2018.01.005
PMID:29339113

2. Ipsen DH, Lykkesfeldt J, Tveden-Nyborg P. Molecular mechanisms of hepatic lipid accumulation in non-alcoholic fatty liver disease. Cell Mol Life Sci. 2018; 75:3313–27.
https://doi.org/10.1007/s00018-018-2860-6
PMID:29936596

3. Tilg H, Adolph TE, Dudek M, Knolle P. Non-alcoholic fatty liver disease: the interplay between metabolism, microbes and immunity. Nat Metab. 2021; 3:1596–607.
https://doi.org/10.1038/s42255-021-00501-9
PMID:34931080

4. Musso G, Gambino R, Cassader M. Cholesterol metabolism and the pathogenesis of non-alcoholic steatohepatitis. Prog Lipid Res. 2013; 52:175–91.
https://doi.org/10.1016/j.plipres.2012.11.002
PMID:23206728

5. Min HK, Kapoor A, Fuchs M, Mirshahi F, Zhou H, Maher J, Kellum J, Warnick R, Contos MJ, Sanyal AJ. Increased hepatic synthesis and dysregulation of cholesterol metabolism is associated with the severity of nonalcoholic fatty liver disease. Cell Metab. 2012; 15:665–74.
https://doi.org/10.1016/j.cmet.2012.04.004
PMID:22560219

6. Deng KQ, Huang X, Lei F, Zhang XJ, Zhang P, She ZG, Cai J, Ji YX, Li H. Role of hepatic lipid species in the progression of nonalcoholic fatty liver disease. Am J Physiol Cell Physiol. 2022; 323:C630–9.
https://doi.org/10.1152/ajpcell.00123.2022
PMID:35759443

7. Ling C, Rönn T. Epigenetics in Human Obesity and Type 2 Diabetes. Cell Metab. 2019; 29:1028–44.
https://doi.org/10.1016/j.cmet.2019.03.009
PMID:30982733

8. Zhang B, Jiang H, Dong Z, Sun A, Ge J. The critical roles of m6A modification in metabolic abnormality and cardiovascular diseases. Genes Dis. 2020; 8:746–58.
https://doi.org/10.1016/j.gendis.2020.07.011
PMID:34522705

9. Dorn LE, Lasman L, Chen J, Xu X, Hund TJ, Medvedovic M, Hanna JH, van Berlo JH, Accornero F. The N[6]-Methyladenosine mRNA Methylase METTL3 Controls Cardiac Homeostasis and Hypertrophy. Circulation. 2019; 139:533–45.
https://doi.org/10.1161/CIRCULATIONAHA.118.036146
PMID:30586742

10. Liu J, Yue Y, Han D, Wang X, Fu Y, Zhang L, Jia G, Yu M, Lu Z, Deng X, Dai Q, Chen W, He C. A METTL3-METTL14 complex mediates mammalian nuclear RNA N6-adenosine methylation. Nat Chem Biol. 2014; 10:93–5.
https://doi.org/10.1038/nchembio.1432
PMID:24316715

11. Pendleton KE, Chen B, Liu K, Hunter OV, Xie Y, Tu BP, Conrad NK. The U6 snRNA m[6]A Methyltransferase METTL16 Regulates SAM Synthetase Intron Retention. Cell. 2017; 169:824–835.e14.
https://doi.org/10.1016/j.cell.2017.05.003
PMID:28525753

12. Ping XL, Sun BF, Wang L, Xiao W, Yang X, Wang WJ, Adhikari S, Shi Y, Lv Y, Chen YS, Zhao X, Li A, Yang Y, et al. Mammalian WTAP is a regulatory subunit of the RNA N6-methyladenosine methyltransferase. Cell Res. 2014; 24:177–89.
https://doi.org/10.1038/cr.2014.3
PMID:24407421

13. Jia G, Fu Y, Zhao X, Dai Q, Zheng G, Yang Y, Yi C, Lindahl T, Pan T, Yang YG, He C. N6-methyladenosine in nuclear RNA is a major substrate of the obesity-associated FTO. Nat Chem Biol. 2011; 7:885–7.
https://doi.org/10.1038/nchembio.687
PMID:22002720

14. Zheng G, Dahl JA, Niu Y, Fedorcsak P, Huang CM, Li CJ, Vågbø CB, Shi Y, Wang WL, Song SH, Lu Z, Bosmans RP, Dai Q, et al. ALKBH5 is a mammalian RNA demethylase that impacts RNA metabolism and mouse fertility. Mol Cell. 2013; 49:18–29.
https://doi.org/10.1016/j.molcel.2012.10.015
PMID:23177736

15. Wang X, Zhao BS, Roundtree IA, Lu Z, Han D, Ma H, Weng X, Chen K, Shi H, He C. N(6)-methyladenosine Modulates Messenger RNA Translation Efficiency. Cell. 2015; 161:1388–99.
https://doi.org/10.1016/j.cell.2015.05.014
PMID:26046440

16. Shi H, Wang X, Lu Z, Zhao BS, Ma H, Hsu PJ, Liu C, He C. YTHDF3 facilitates translation and decay of N^6-methyladenosine-modified RNA. Cell Res. 2017; 27:315–28.
https://doi.org/10.1038/cr.2017.15
PMID:28106072

17. Huang H, Weng H, Sun W, Qin X, Shi H, Wu H, Zhao BS, Mesquita A, Liu C, Yuan CL, Hu YC, Hüttelmaier S, Skibbe JR, et al. Recognition of RNA N^6-methyl-adenosine by IGF2BP proteins enhances mRNA stability and translation. Nat Cell Biol. 2018; 20:285–95.
https://doi.org/10.1038/s41556-018-0045-z
PMID:29476152

18. Zhao BS, Roundtree IA, He C. Post-transcriptional gene regulation by mRNA modifications. Nat Rev Mol Cell Biol. 2017; 18:31–42.
https://doi.org/10.1038/nrm.2016.132
PMID:27808276

19. Lin Z, Hsu PJ, Xing X, Fang J, Lu Z, Zou Q, Zhang KJ, Zhang X, Zhou Y, Zhang T, Zhang Y, Song W, Jia G, et al. Mettl3-/Mettl14-mediated mRNA N^6-methyladenosine modulates murine spermato-genesis. Cell Res. 2017; 27:1216–30.
https://doi.org/10.1038/cr.2017.117
PMID:28914256

20. Batista PJ, Molinie B, Wang J, Qu K, Zhang J, Li L, Bouley DM, Lujan E, Haddad B, Daneshvar K, Carter AC, Flynn RA, Zhou C, et al. m(6)A RNA modification controls cell fate transition in mammalian embryonic stem cells. Cell Stem Cell. 2014; 15:707–19.
https://doi.org/10.1016/j.stem.2014.09.019
PMID:25456834

21. Xu Y, Zhou Z, Kang X, Pan L, Liu C, Liang X, Chu J, Dong S, Li Y, Liu Q, Sun Y, Yu S, Zhang Q. Mettl3-mediated mRNA m^6A modification controls postnatal liver development by modulating the transcription factor Hnf4a. Nat Commun. 2022; 13:4555.
https://doi.org/10.1038/s41467-022-32169-4
PMID:35931692

22. Chen M, Wei L, Law CT, Tsang FH, Shen J, Cheng CL, Tsang LH, Ho DW, Chiu DK, Lee JM, Wong CC, Ng IO, Wong CM. RNA N6-methyladenosine methyltransferase-like 3 promotes liver cancer progression through YTHDF2-dependent posttranscriptional silencing of SOCS2. Hepatology. 2018; 67:2254–70.
https://doi.org/10.1002/hep.29683
PMID:29171881

23. Li X, Yuan B, Lu M, Wang Y, Ding N, Liu C, Gao M, Yao Z, Zhang S, Zhao Y, Xie L, Chen Z. The methyltransferase METTL3 negatively regulates nonalcoholic steatohepatitis (NASH) progression. Nat Commun. 2021; 12:7213.
https://doi.org/10.1038/s41467-021-27539-3
PMID:34893641

24. Barajas JM, Lin CH, Sun HL, Alencastro F, Zhu AC, Aljuhani M, Navari L, Yilmaz SA, Yu L, Corps K, He C, Duncan AW, Ghoshal K. METTL3 Regulates Liver Homeostasis, Hepatocyte Ploidy, and Circadian Rhythm-Controlled Gene Expression in Mice. Am J Pathol. 2022; 192:56–71.
https://doi.org/10.1016/j.ajpath.2021.09.005
PMID:34599880

25. Qin Y, Li B, Arumugam S, Lu Q, Mankash SM, Li J, Sun B, Li J, Flavell RA, Li HB, Ouyang X. m^6A mRNA methylation-directed myeloid cell activation controls progression of NAFLD and obesity. Cell Rep. 2021; 37:109968.
https://doi.org/10.1016/j.celrep.2021.109968
PMID:34758326

26. Rada P, González-Rodríguez Á, García-Monzón C, Valverde ÁM. Understanding lipotoxicity in NAFLD pathogenesis: is CD36 a key driver? Cell Death Dis. 2020; 11:802.
https://doi.org/10.1038/s41419-020-03003-w
PMID:32978374

27. Qi J, Lang W, Geisler JG, Wang P, Petrounia I, Mai S, Smith C, Askari H, Struble GT, Williams R, Bhanot S, Monia BP, Bayoumy S, et al. The use of stable isotope-labeled glycerol and oleic acid to differentiate the hepatic functions of DGAT1 and -2. J Lipid Res. 2012; 53:1106–16.
https://doi.org/10.1194/jlr.M020156
PMID:22493088

28. Villanueva CJ, Monetti M, Shih M, Zhou P, Watkins SM, Bhanot S, Farese RV Jr. Specific role for acyl

CoA:Diacylglycerol acyltransferase 1 (Dgat1) in hepatic steatosis due to exogenous fatty acids. Hepatology. 2009; 50:434–42.
https://doi.org/10.1002/hep.22980
PMID:19472314

29. Wurie HR, Buckett L, Zammit VA. Diacylglycerol acyltransferase 2 acts upstream of diacylglycerol acyltransferase 1 and utilizes nascent diglycerides and de novo synthesized fatty acids in HepG2 cells. FEBS J. 2012; 279:3033–47.
https://doi.org/10.1111/j.1742-4658.2012.08684.x
PMID:22748069

30. Weber M, Mera P, Casas J, Salvador J, Rodríguez A, Alonso S, Sebastián D, Soler-Vázquez MC, Montironi C, Recalde S, Fucho R, Calderón-Domínguez M, Mir JF, et al. Liver CPT1A gene therapy reduces diet-induced hepatic steatosis in mice and highlights potential lipid biomarkers for human NAFLD. FASEB J. 2020; 34:11816–37.
https://doi.org/10.1096/fj.202000678R
PMID:32666604

31. Allali-Hassani A, Peralba JM, Martras S, Farrés J, Parés X. Retinoids, omega-hydroxyfatty acids and cytotoxic aldehydes as physiological substrates, and H2-receptor antagonists as pharmacological inhibitors, of human class IV alcohol dehydrogenase. FEBS Lett. 1998; 426:362–6.
https://doi.org/10.1016/s0014-5793(98)00374-3
PMID:9600267

32. Liu H, Pathak P, Boehme S, Chiang JL. Cholesterol 7α-hydroxylase protects the liver from inflammation and fibrosis by maintaining cholesterol homeostasis. J Lipid Res. 2016; 57:1831–44.
https://doi.org/10.1194/jlr.M069807
PMID:27534992

33. Bao LD, Li CQ, Peng R, Ren XH, Ma RL, Wang Y, Lv HJ. Correlation between the decrease of cholesterol efflux from macrophages in patients with type II diabetes mellitus and down-regulated CYP7A1 expression. Genet Mol Res. 2015; 14:8716–24.
https://doi.org/10.4238/2015.July.31.20
PMID:26345803

34. Chen Y, Chen Y, Zhao L, Chen Y, Mei M, Li Q, Huang A, Varghese Z, Moorhead JF, Ruan XZ. Inflammatory stress exacerbates hepatic cholesterol accumulation via disrupting cellular cholesterol export. J Gastroenterol Hepatol. 2012; 27:974–84.
https://doi.org/10.1111/j.1440-1746.2011.06986.x
PMID:22098164

35. Wang J, Mitsche MA, Lütjohann D, Cohen JC, Xie XS, Hobbs HH. Relative roles of ABCG5/ABCG8 in liver and intestine. J Lipid Res. 2015; 56:319–30.
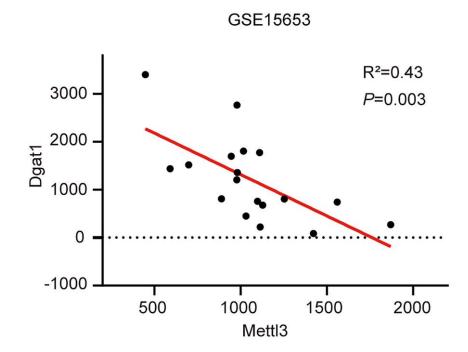https://doi.org/10.1194/jlr.M054544
PMID:25378657

36. Jiang SY, Li H, Tang JJ, Wang J, Luo J, Liu B, Wang JK, Shi XJ, Cui HW, Tang J, Yang F, Qi W, Qiu WW, Song BL. Discovery of a potent HMG-CoA reductase degrader that eliminates statin-induced reductase accumulation and lowers cholesterol. Nat Commun. 2018; 9:5138.
https://doi.org/10.1038/s41467-018-07590-3
PMID:30510211

37. Lee Y, Choe J, Park OH, Kim YK. Molecular Mechanisms Driving mRNA Degradation by m^6A Modification. Trends Genet. 2020; 36:177–88.
https://doi.org/10.1016/j.tig.2019.12.007
PMID:31964509

38. Lin X, Jia J, Du T, Li W, Wang X, Wei J, Lin X, Zeng H, Yao L, Chen X, Zhuang J, Weng J, Liu Y, et al. Overexpression of miR-155 in the liver of transgenic mice alters the expression profiling of hepatic genes associated with lipid metabolism. PLoS One. 2015; 10:e0118417.
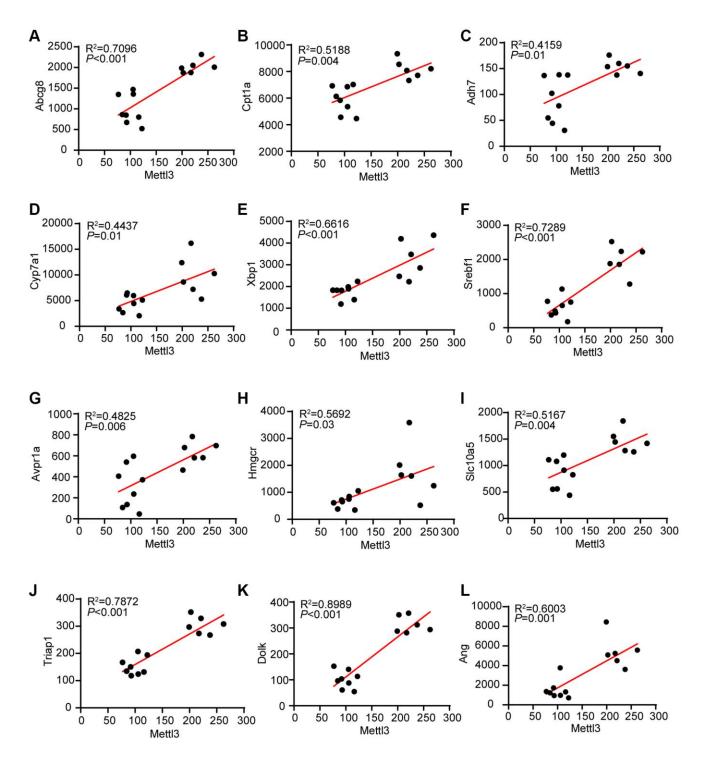https://doi.org/10.1371/journal.pone.0118417
PMID:25799309

39. Bertola A, Mathews S, Ki SH, Wang H, Gao B. Mouse model of chronic and binge ethanol feeding (the NIAAA model). Nat Protoc. 2013; 8:627–37.
https://doi.org/10.1038/nprot.2013.032
PMID:23449255

40. Charlton M, Krishnan A, Viker K, Sanderson S, Cazanave S, McConico A, Masuoko H, Gores G. Fast food diet mouse: novel small animal model of NASH with ballooning, progressive fibrosis, and high physiological fidelity to the human condition. Am J Physiol Gastrointest Liver Physiol. 2011; 301:G825–34.
https://doi.org/10.1152/ajpgi.00145.2011
PMID:21836057

41. Subramanian A, Tamayo P, Mootha VK, Mukherjee S, Ebert BL, Gillette MA, Paulovich A, Pomeroy SL, Golub TR, Lander ES, Mesirov JP. Gene set enrichment analysis: a knowledge-based approach for interpreting genome-wide expression profiles. Proc Natl Acad Sci U S A. 2005; 102:15545–50.
https://doi.org/10.1073/pnas.0506580102
PMID:16199517

42. Robinson JT, Thorvaldsdóttir H, Winckler W, Guttman M, Lander ES, Getz G, Mesirov JP. Integrative genomics viewer. Nat Biotechnol. 2011; 29:24–6.
https://doi.org/10.1038/nbt.1754
PMID:21221095

43. Zhou Y, Zeng P, Li YH, Zhang Z, Cui Q. SRAMP: prediction of mammalian N6-methyladenosine (m6A) sites based on sequence-derived features. Nucleic Acids Res. 2016; 44:e91.
https://doi.org/10.1093/nar/gkw104
PMID:26896799

Supplementary Figures

GSE15653

R²=0.43
P=0.003

Supplementary Figure 1. The expression of Mettl3 is significantly negatively correlated with Dgat1 in GEO datasets.

Supplementary Figure 2. The expression correlation of the potential downstream target genes with Mettl3. (**A**) The correlation between Abcg8, Cpt1a (**B**), Adh7 (**C**), Cyp7a1 (**D**), Xbp1 (**E**), Srebf1 (**F**), Avpr1a (**G**), Hmgcr (**H**), Slc10a5 (**I**), Triap1 (**J**), Dolk (**K**), Ang (**L**) expression and Mettl3 expression was determined by Pearson's correlation test from liver mRNA profiles of 5-week-old wild type and Mettl3 liver specific knockout mice in a GEO datasets (GSE176113).

Supplementary Table

Supplementary Table 1. Primers for qRT-PCR analysis of lipid metabolism genes.

Gene	Forward primer (5′–3′)	Reverse primer (5′–3′)
Gapdh	CCTGCTTCACCACCTTCTTG	CATGGCCTTCCGTGTTCCTA
Mettl3	ATCCAGGCCCATAAGAAACAG	CTATCACTACGGAAGGTTGGG
Cd36	ATGGGCTGTGATCGGAACTG	GTCTTCCCAATAAGCATGTCTCC
Cyp7a1	GGGATTGCTGTGGTAGTGAGC	GGTATGGAATCAACCCGTTGTC
Abcg8	CTGTGGAATGGGACTGTACTTC	GTTGGACTGACCACTGTAGGT
Hmgcr	AGCTTGCCCGAATTGTATGTG	TCTGTTGTGAACCATGTGACTTC
Adh7	ATGGGCACCGCTGGAAAAG	TAACACGGACTTCCTTAGCCT
Cpt1a	CTCCGCCTGAGCCATGAAG	CACCAGTGATGATGCCATTCT
Srebf1	TGACCCGGCTATTCCGTGA	CTGGGCTGAGCAATACAGTTC
Avpr1a	TGAGTTTCGTTCTGAGCATACC	CCCAGCAATCTTGGGCTTTG
Rdh16f2	TCTTGGGCAGAGTGTCACTTG	TGCCAGGTATTTCTCTCCATAGA
Slc10a5	CAGCTACCTGCTCGTGAAGTT	AGGTTGACGGTAAAGTCTGTGA
Triap1	GAGTACGACCAGTGCTTCAAC	CTTGATTGCTTTCTGCACGCA
Xbp1	AGCAGCAAGTGGTGGATTTG	GAGTTTTCTCCCGTAAAAGCTGA
Dolk	CAGTGTGGGACCGATACTCCT	CCAAGCAAAGGCATGACCA
Ang	CCAGGCCCGTTGTTCTTGAT	GGAAGGGAGACTTGCTCATTC
Acaa1a	TCTCCAGGACGTGAGGCTAAA	CGCTCAGAAATTGGGCGATG
Acaa2	CTGCTACGAGGTGTGTTCATC	AGCTCTGCATGACATTGCCC
Acad11	TGACACCGTGGAAGTGCTAC	CCCGGCAAGTGCTGATTCA
Abcd3	GGCCTGCACGGTAAGAAAAGT	CCGCAATAAGTAACAAGTAGCCT
Bdh2	CGACTGGACGGCAAAGTTATT	CCTGGAGTTTGGACTCGTTGA
Apoa2	TGGTCGCACTGCTGGTAAC	TTTGCCATATTCAGTCATGCTCT
Apoa5	TCCTCGCAGTGTTCGCAAG	CGAAGCTGCCTTTCAGGTTCT
Apof	ATAGCCTCCGACTCATCCTGA	TCTGCATCTGGTATCCCAACTT
Ceslb	TACCTCCCCTGTTTTCCGAAG	GATGCTCCGCCTGTCATCAAT
Cesld	ATGCGCCTCTACCCTCTGATA	AGCAAATCTCAAGGAGCCAAG
Cesle	CAACTTCTGGAATTGATTGGGGA	GGGCTCCGGCATCTCTATG